A longitudinal gradient of synaptic drive in the spinal cord of *Xenopus* embryos and its role in co-ordination of swimming

Mark J. Tunstall and Alan Roberts*

School of Biological Sciences, University of Bristol, Woodland Road, Bristol BS8 1UG

1. Intersegmental co-ordination in *Xenopus* embryos could be influenced by longitudinal gradients in neuronal properties or synaptic drive. To determine if such gradients exist intracellular recordings were made from putative motoneurones at different spinal levels.

2. No evidence was found of a longitudinal gradient in neuronal resting potentials. In a rostrocaudal direction the duration of current-evoked spikes increased and the amplitude of the spike after-hyperpolarization (AHP) decreased.

3. During fictive swimming the amplitude of the tonic excitatory synaptic input and the mid-cycle IPSPs declined in a rostrocaudal direction. The rise-time and fall-time of mid-cycle IPSPs increased in a rostrocaudal direction.

4. Rostral to the eighth post-otic segment mid-cycle IPSPs occurred on all cycles of fictive swimming episodes. More caudally IPSPs became irregular in occurrence and caudal to the twelfth post-otic segment no mid-cycle IPSPs could be detected, even during the injection of depolarizing current or when recording with KCl-filled electrodes.

5. The duration of spikes occurring during fictive swimming increased and the amplitude of spike AHP decreased in a rostrocaudal direction. A spike AHP was absent during fictive swimming activity in neurones caudal to the ninth post-otic segment even though it was present in current-evoked spikes in the same neurones.

6. On-cycle IPSPs (occurring shortly after the spike at phase values less than 0·4) were observed predominantly at the beginning of swimming episodes in neurones recorded rostral to the eighth segment, but were not detected at all in more caudal neurones.

7. If the rostrocaudal gradients in synaptic excitatory and inhibitory drive to putative motoneurones during fictive swimming are also present in premotor spinal interneurones they would be expected to have a strong influence on rostrocaudal delays. Such gradients could therefore be important components of the mechanism underlying intersegmental co-ordination.

During swimming in a wide range of animals, including leeches, fish, amphibian embryos and tadpoles, alternating waves of bending pass along the body from head to tail. The generation of these waves of bending can be attributed to an underlying pattern of muscular and neural activity that alternates between opposite sides (intrasegmental co-ordination) and travels in a head-to-tail (rostrocaudal) direction along the body (intersegmental co-ordination). In a range of swimming animals it has been shown that the central nervous system has intersegmental co-ordination mechanisms which can generate a rostrocaudal wave of motor activity suitable for producing swimming without reflexes (leech: Pearce & Friesen, 1984; lamprey: Wallen & Williams, 1982; dogfish: Grillner, Perret & Zangger, 1976; *Xenopus*: Roberts, 1990). In the crayfish central nervous system intersegmental co-ordination mechanisms exist to control the caudorostral wave of swimmeret movements (Ikeda & Wiersma, 1964).

For the swimming animals mentioned, considerable progress has been made in understanding the neurones and mechanisms underlying intrasegmental co-ordination (leech: Friesen, 1989; lamprey: Grillner, Buchanan, Wallen & Brodin, 1988; *Xenopus* embryos: Roberts, 1990). In contrast, the mechanisms underlying intersegmental co-ordination, which introduce delays between activity at the front and back, are less well understood.

Since some degree of distributed rhythm-generating capacity has generally been demonstrated (crayfish swimmeret system: Ikeda & Wiersma, 1964; Paul & Mulloney, 1986; leech: Pearce & Friesen, 1985*a*, *b*; lamprey: Cohen & Wallen, 1980; *Xenopus* embryo: Kahn & Roberts, 1982; Roberts & Alford, 1986), a common approach used to

*To whom correspondence should be addressed.

investigate intersegmental co-ordination is to view the central nervous circuitry as a population of coupled oscillators (Pavlidis, 1973). Experimental and theoretical studies have suggested two mechanisms that determine the magnitude and direction of longitudinal intersegmental delays. Firstly, co-ordination may depend on a longitudinal difference in the intrinsic frequency of a population of coupled oscillators (lamprey: Grillner, 1974; Cohen, Holmes & Rand, 1982; Grillner *et al.* 1988). Such longitudinal differences in frequency were not found in the lamprey (Cohen, 1987) but in the leech, where only the first sixteen segments out of thirty-two can generate rhythm, the oscillator frequency increases caudally within the first sixteen segments (Pearce & Friesen, 1985*a*, *b*). Secondly, intersegmental co-ordination depends on the nature of the coupling between the oscillators (crayfish swimmeret system: Stein, 1976; Paul & Mulloney, 1986; lamprey: Rovainen, 1986; Kopell, 1988; Buchanan, 1992; Williams, 1992). The difficulty here has been to obtain direct evidence about the nature of axonal projections and synaptic strengths of neurones mediating such coupling. Direct paired recordings from individual neurones are very difficult, but necessary to give a general picture (Dale & Roberts, 1984; Buchanan, Grillner, Cullheim & Risling, 1989). Experiments like those of Williams, Kopell, Sigvardt, Ermentrout & Remler (1990) provide indirect evidence about the coupling.

Recently we proposed a gradient hypothesis to explain intersegmental co-ordination during swimming in *Xenopus* embryos (Tunstall & Roberts, 1990, 1991*a*, *b*). We suggested that rostrocaudal delays may result from a gradient in neuronal excitability along the spinal circuitry. Since the premotor interneurones active in swimming are present at higher densities rostrally and only project for a few segments (Roberts & Alford, 1986; Roberts, Dale, Ottersen & Storm-Mathisen, 1988), rostral neurones might be expected to have stronger synaptic input resulting in higher excitability. This synaptic input from premotor interneurones drives the oscillations of swimming and provides a signal to couple oscillations in neighbouring segments. As a consequence more rostral regions with stronger synaptic drive may have higher intrinsic frequencies of oscillation and stronger interoscillator coupling. Our experiments showed that caudal application of excitants decreased rostrocaudal delay, while application of excitatory antagonists increased it. Such results are compatible with the notion that the spinal circuitry is organized as a population of coupled oscillators. Similar experiments have been performed by Matsushima & Grillner (1990, 1992) for agonist-induced fictive swimming in the lamprey spinal cord preparation. They have shown that any segmental oscillator which has the highest frequency (usually as a result of treatment with the highest concentration of excitant) can entrain adjacent oscillators to the same frequency but with a phase delay. Thus in both the *Xenopus* embryo and the lamprey, artificial imposed gradients can influence intersegmental co-ordination, but we still do not know how this occurs naturally.

If a longitudinal gradient in cellular properties or in the synaptic drive to rhythmically active neurones during fictive swimming contributes to intersegmental co-ordination the first step is to obtain evidence for the existence of such gradients. In this study we have recorded intracellularly from putative motoneurones at different spinal positions and looked for longitudinal variation in their properties and the levels of synaptic drive that they receive during fictive swimming activity. Longitudinal variation in motoneurone properties might indicate that variation could also occur in interneurones. The levels of excitatory and inhibitory synaptic drive to the motoneurones should indicate whether there is longitudinal variation in synaptic output from premotor interneurones. A preliminary report of some aspects of this work has been published (Tunstall & Roberts, 1991*a*).

METHODS

Experiments were performed on *Xenopus* embryos at developmental stage 37/38 (Nieuwkoop & Faber, 1956). Prior to experimentation embryos were anaesthetized in MS-222, and the dorsal fin was slit along its length to facilitate access of the neuromuscular blocker α-bungarotoxin (10 μM), into which they were placed after recovery from anaesthesia. Animals were left until they no longer displayed activity in response to normally effective stimuli. The embryos were then secured on their sides to the Sylgard surface of a rotatable Perspex platform located within a preparation bath. In all experiments preparations were perfused by saline solution (composition (mM): Na^+, 115; K^+, 2·5; Ca^{2+}, 4·0; Mg^{2+}, 1·0; Cl^-, 108·5; HCO_3^-, 15), which was buffered to pH 7·2 with 5% O_2 and 95% CO_2 (Soffe, 1989). Mg^{2+} was present at physiological levels and not as a calcium channel blocker. The trunk skin overlying the myotomes was removed using fine pins. Extracellular recordings from ventral roots were made by placing a suction electrode over an intersegmental cleft at variable positions between the third and seventh post-otic segments. To enable intracellular recordings to be made the myotomes overlying the spinal cord were removed from the level of the otic capsule to the level of the fifteenth post-otic segment. Neurones were impaled using glass microelectrodes, which were filled with either 3 M potassium acetate or 2 M potassium chloride and had DC resistances of 150–350 MΩ. By recording in the ventral quarter of the cord the probability of recording from motoneurones is very high, as anatomical studies have shown this region contains very few interneurones (Roberts & Clarke, 1982; Soffe & Roberts, 1982*a*). Normal swimming activity was evoked by a 1 ms current pulse, applied via a glass suction electrode (50 μm tip opening), to the ipsilateral tail skin of the quiescent preparation at about the level of the anus. Signals were stored on magnetic tape and later captured using a CED 1401 analog-to-digital interface in conjunction with CED SPIKE2 software (Cambridge Electronic Design, Cambridge, UK), the latter also being used to analyse the signals and, in conjunction with a Hewlett-Packard X–Y plotter, to make permanent records. The data presented here are based on recordings from thirty-two ventral neurones at longitudinal positions along the spinal cord from the second to the fourteenth post-otic segments in twenty-five preparations. For seventeen of these neurones, spike properties were examined during swimming and in response to current injection. The point of entry of the microelectrode into the spinal cord was used to

define the approximate position of an impaled motoneurone. Lines of linear regression were determined using the least-squares method. Curve fitting of spike falling phases was performed using the Marquardt–Levenberg least-squares algorithm.

RESULTS

Longitudinal variation of resting potentials and of current-evoked spike features

In this section we describe the measurements made of resting potentials and the magnitudes of some features of just-superthreshold current-evoked spikes. Recordings were made from ventral, putative motoneurones at different longitudinal positions in unstimulated embryos at rest and using potassium acetate-filled microelectrodes.

Resting potentials

The resting potential of putative motoneurones was determined as the difference between the stable potential attained during impalement and the small potential which often remained immediately after withdrawal of the electrode. Resting potentials ranged from −55 to −90 mV (mean -74 ± 5 mV, $n = 32$) but no significant longitudinal trend was found ($P > 0{\cdot}05$).

Spike features

Measurements in this section are based on recordings from seventeen putative motoneurones from seventeen different animals. In response to sustained depolarizing current injection putative motoneurones usually fired only a single, non-overshooting spike at just-superthreshold current ($n = 14$, Fig. 1*A*) although in a small number of putative motoneurones up to three spikes were fired ($n = 3$). This tendency to exhibit membrane accommodation is consistent with the findings of Soffe (1990) and may be due to the effects of one or more types of K^+ channel since putative motoneurones can fire repetitively when recorded with microelectrodes containing Cs^{2+}, a blocker of K^+ channels (Soffe, 1990). The peak spike amplitude (V_{peak}, Fig. 1*B*) and the amplitude of the spike threshold ($V_{threshold}$, Fig. 1*B*) were determined for putative motoneurones recorded at different longitudinal positions. Peak spike amplitudes ranged from 66 to 98 mV (mean $80{\cdot}82 \pm 8{\cdot}12$ mV) and the amplitude of the thresholds ranged from 23 to 39 mV (mean $38 \pm 4{\cdot}73$ mV). Neither of these parameters varied significantly with spinal position ($P > 0{\cdot}05$).

We examined a number of other features of current-evoked spikes to see if significant longitudinal differences existed which could influence intersegmental delays. The amplitude of the spike after-hyperpolarization (V_{AHP}, Fig. 2*A*) decreased significantly in a rostrocaudal direction ($P < 0{\cdot}05$; Fig. 2*B*). Spike durations, which were measured at half peak amplitude (*d*, Fig. 2*A*), increased significantly in a rostrocaudal direction ($P < 0{\cdot}05$, Fig. 2*C*). Input resistances were calculated by dividing the steady-state membrane potential (V_{ss}) by the current (I_{ss}) (Fig. 2*A*). Input resistances ranged from 50 to 125 MΩ, but no significant longitudinal variation was found ($P > 0{\cdot}05$, Fig. 2*D*). These results indicate that, compared to rostral neurones, current-evoked spikes in caudal neurones have longer durations and smaller amplitude AHPs.

Longitudinal variation in synaptic drive and spike features during fictive swimming

We now turn our attention towards looking for the existence of longitudinal differences in the properties of the spikes and synaptic drive which occur during fictive

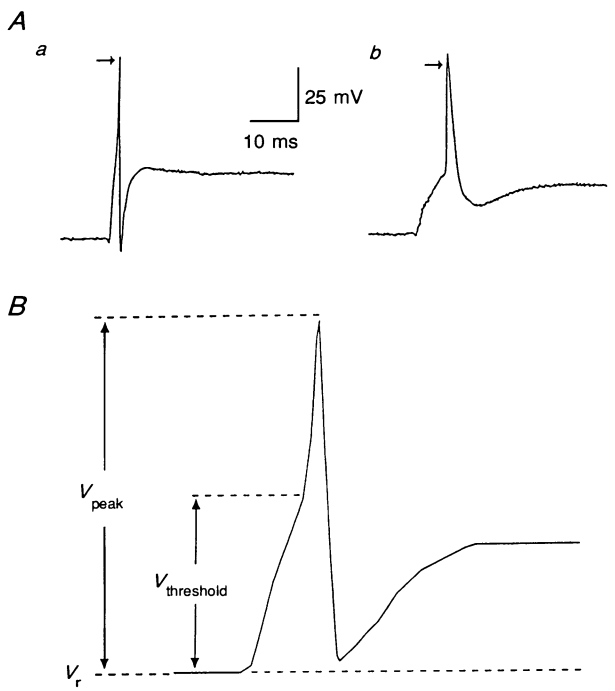

Figure 1. Examples of current-evoked spikes and definitions of spike features
A, just-superthreshold current-evoked spikes recorded from: *a*, segment 5 in response to 0·54 nA of current; and *b*, segment 10 in response to 0·43 nA of current. *B*, diagram of a current-evoked spike to show the measurements made of spike features. V_r is the resting potential, V_{peak} is the peak spike amplitude and $V_{threshold}$ is the amplitude of the spike threshold. The arrows in *A* indicate 0 mV.

swimming. Intracellular recordings were made from putative motoneurones using either potassium acetate- or potassium chloride-filled electrodes during swimming episodes evoked by applying a brief electrical stimulus to the tail skin. For each of the thirty-two neurones recorded, six swimming episodes were used for analysis and the following procedure was adopted. During fictive swimming episodes in *Xenopus* embryos frequency decreases (Roberts & Kahn, 1982). Thus, for each component of the swimming activity investigated, measurements were made over each of four frequency ranges (11·5–13·5, 13·5–15·5, 15·5–17·5 and 17·5–19·5 Hz), chosen to encompass the entire range of frequencies expressed by all the swimming episodes measured. Each component was measured on all cycles of swimming within each frequency range. Linear regression analysis was used to check that there was no significant trend in the values of each component within each frequency range; no such trend was found ($P > 0·05$). For each frequency range the data from the six swimming episodes were compared using analysis of variance in order to ensure that there was no significant difference between the six data sets. No such difference was detected on any occasion ($P > 0·05$). An overall mean was then determined based on the pooled data from all the six swimming episodes measured. For each frequency range linear regression was used to determine whether there was a significant relationship between the measured components and longitudinal position. To check that the slopes of these regression lines were not significantly different for each frequency range, analysis of covariance was used. No significant difference was found ($P > 0·05$), and in view of this the data for all the components measured in the following sections refers to a single representative frequency range (13·5–15·5 Hz), which was the mean range found over all the swimming episodes measured. In all episodes this frequency range was achieved 500 ms after the start of swimming, thus eliminating the possibility that our results may be influenced by the initiating sensory stimulus applied to the tail since the sensory postsynaptic potentials should be over by this time (Sillar & Roberts, 1988).

Synaptic drive

During fictive swimming membrane potentials of rhythmically active motoneurones (Roberts & Kahn, 1982; Soffe & Roberts, 1982*a*; Dale & Roberts, 1984) and interneurones (Soffe, Clarke & Roberts, 1984; Dale, 1985; Dale & Roberts, 1985) are tonically depolarized from the resting potential and the single spikes fired on each cycle are separated at mid-cycle by hyperpolarizing, inhibitory postsynaptic potentials (IPSPs). There are three principal components underlying this pattern of swimming activity: the cycle-by-

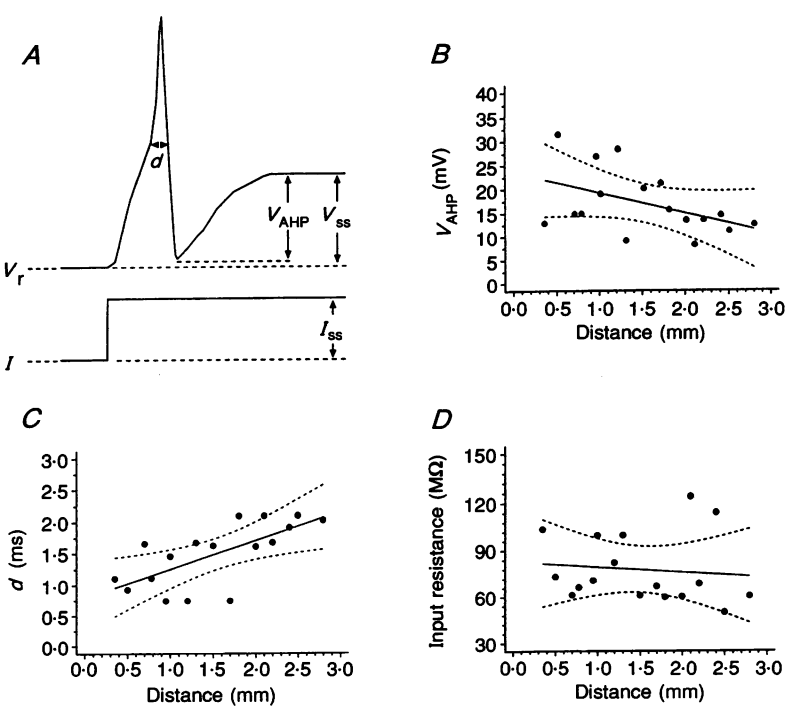

Figure 2. The definition of some spike features and the relationship between these features and spinal position

A, V_{AHP} is the amplitude of the spike after-hyperpolarization and *d* is the spike duration measured at the point of half peak amplitude. The relationship between spinal position and V_{AHP} (*B*) and spike duration (*d*, panel *C*) is significant ($P < 0·05$). In *D*, input resistance, which is calculated by dividing the amplitude of the steady-state potential (V_{ss}) by the steady-state current (I_{ss}), does not vary significantly with spinal position ($P > 0·05$). In *B*, *C* and *D*, the dashed lines indicate the 95% confidence limits associated with the line of linear regression.

cycle summation of slow, NMDA-mediated potentials, which gives rise to the tonic depolarization (Dale & Roberts, 1985); the fast kainate/quisqualate potentials, which underlie the spikes fired on each cycle (Dale & Roberts, 1985); and the glycine-dependent mid-cycle IPSPs (Dale, 1985; Soffe, 1987). Our investigations have focused on the amplitude of the tonic depolarization and the amplitude and time course of the mid-cycle IPSPs; no measurements have been made of the fast component.

Recordings from different longitudinal levels revealed a clear rostrocaudal decline in the amplitude of the tonic depolarization and the mid-cycle IPSPs (Fig. 3). To evaluate these trends numerically we measured the amplitude of the tonic depolarization and the amplitude and time course of the mid-cycle IPSPs. Tonic depolarization amplitudes were measured at a cycle phase of 0·4, a point when the fast component would be expected to be very small (Dale & Roberts, 1985) and the amplitude of the mid-cycle IPSPs was measured from the point of take-off to the peak (Fig. 4*A*). IPSP rise-times were measured from the time of take-off to the time of the peak and fall-times were measured from the time of the peak to the time of half-fall (indicated by the dotted and dashed lines respectively in Fig. 4*A*).

The decline in amplitude of the tonic depolarization was linear and significant ($P < 0·05$), with amplitudes ranging from a maximum of approximately 30 mV rostrally to a minimum of 10 mV caudally (Fig. 4*Ba*).

Whereas prominent mid-cycle IPSPs were present during activity recorded from rostrally located putative motoneurones they appeared to be absent for neurones recorded caudal to the twelfth post-otic segment (Fig. 3). In between these two extremes mid-cycle IPSPs tended to decline in amplitude in a linear fashion with spinal position, this rostrocaudal decline being significant ($P < 0·05$, Fig. 4*Bb*).

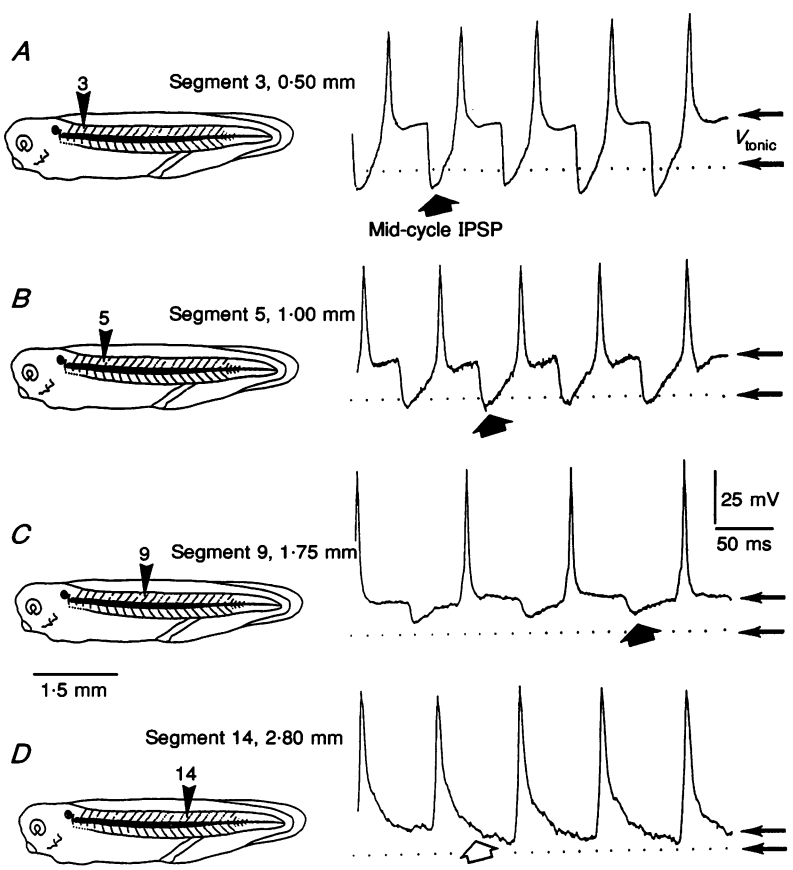

Figure 3. Activity recorded from motoneurones at different spinal positions
The vertical arrowheads indicate the position along the spinal cord from which recordings were made; the numbers above the arrowheads are the corresponding segment numbers. Positions are also indicated in terms of segment number and distance from the otic capsule (e.g. a recording made at the level of the fifth post-otic segment at a distance of 1·00 mm from the midbrain is given as segment 5, 1·00 mm). The distance between the pair of horizontal arrows at the right of each voltage–time curve is proportional to the amplitude of the tonic depolarization. The filled arrows indicate the mid-cycle IPSPs and the open arrow in the lowermost record indicates the expected position of a mid-cycle IPSP. Note that there is a rostrocaudal decline in the amplitude of the tonic depolarization, V_{tonic}, and a decrease in the amplitude of the mid-cycle IPSPs. In *D*, IPSPs are absent where activity was recorded from extreme caudal positions.

There was also a significant ($P < 0.05$) rostrocaudal increase in the rise-time (Fig. 4*Bc*) and fall-time (Fig. 4*Bd*) of the mid-cycle IPSPs. Taken together these findings indicate that mid-cycle IPSPs become smaller in amplitude and longer in duration in a rostrocaudal direction.

As well as the longitudinal decline in the amplitude of the mid-cycle IPSPs there was also a tendency for mid-cycle IPSPs to be absent on some cycles of swimming episodes recorded caudal to the eighth post-otic segment (Fig. 5). On those cycles where they did occur their amplitudes ranged from 2 to 30 mV, rise-times from 6 to 10 ms and fall-times from 12 to 15 ms. Numerically the reliability of mid-cycle IPSP occurrence for a given swimming episode was expressed as the percentage of the total number of cycles of the swimming episode on which an IPSP occurred (Fig. 5*B*). Mid-cycle IPSPs occurred on all cycles of swimming episodes recorded rostral to the ninth post-otic segment, but more caudally reliability decreased markedly. Mid-cycle IPSPs were absent for swimming episodes recorded caudal to the twelfth post-otic segment.

There is strong evidence that the mid-cycle IPSPs occur due to the action of glycine increasing conductance to Cl^- (Roberts & Kahn, 1982; Soffe, 1987). In view of this a possible explanation for the apparent absence of mid-cycle IPSPs in neurones recorded caudal to the twelfth segment is that membrane potentials were close to the Cl^- reversal potential. To investigate this possibility two strategies were used. The first was to inject neurones with pulses of depolarizing

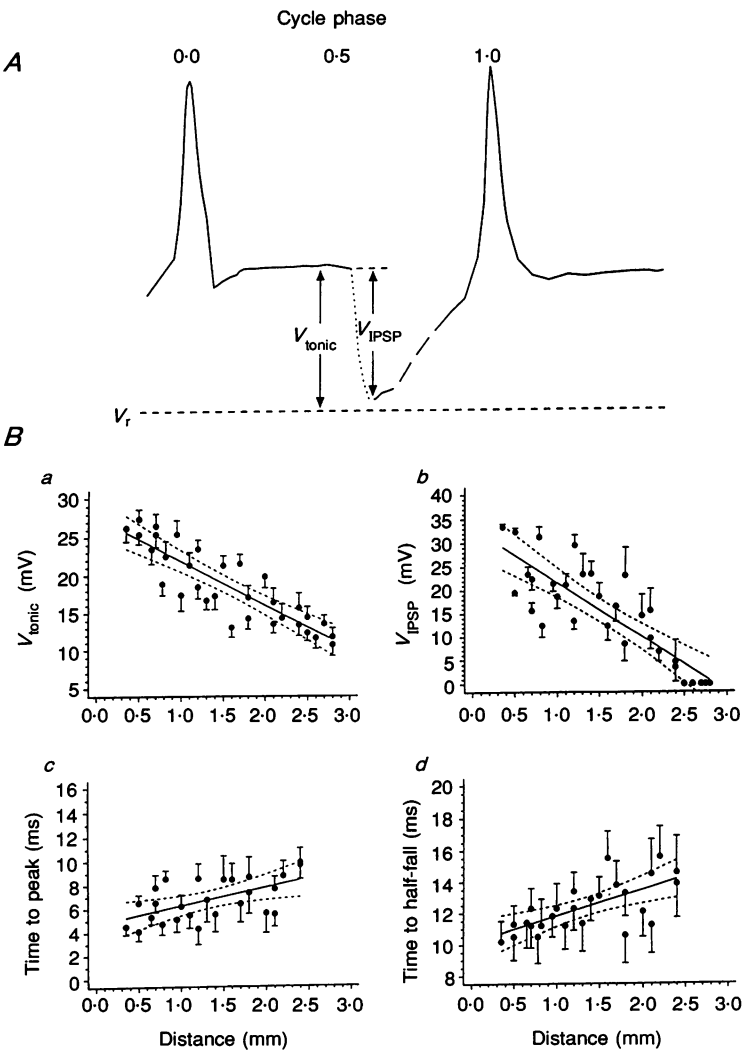

Figure 4. Definitions of the amplitude of the tonic depolarization and the features of the mid-cycle IPSPs and their relationship with spinal position

A, the amplitude of the tonic depolarization (V_{tonic}) was measured relative to the resting potential (V_r) at a cycle phase of 0·4. The amplitude of the mid-cycle IPSPs (V_{IPSP}) was measured from the point of take-off of the IPSP to its peak. The dotted line indicates the rising phase of the IPSP and the dashed line indicates the falling phase to the point of half-fall. *B*, graphs showing the relationship between spinal position and the amplitude of the tonic depolarization (*a*), and the amplitude (*b*), time to peak (*c*) and time to half-fall (*d*) of the mid-cycle IPSPs. In all cases the error bars are the S.D. and the dashed lines are the 95 % confidence limits for the regression line.

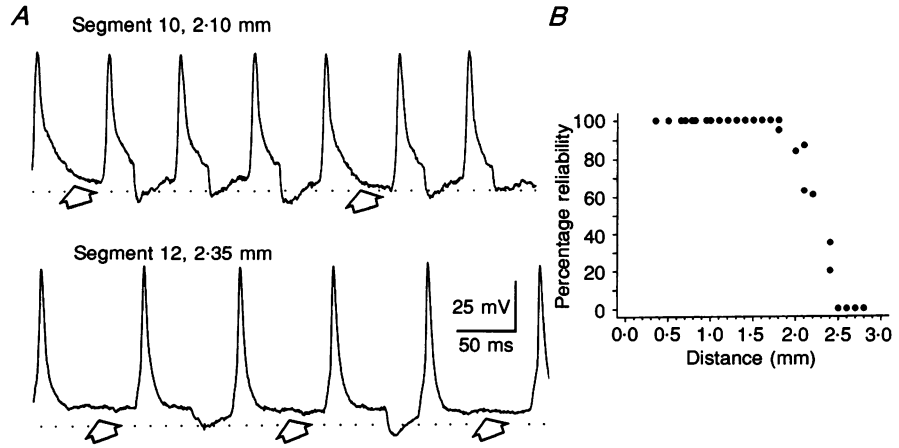

Figure 5. The reliability of occurrence of mid-cycle IPSPs
A, in two motoneurones, one recorded at segment 10 and the other at segment 12, mid-cycle IPSPs do not occur on the cycles of swimming indicated by the open arrowheads. *B*, the reliability of occurrence of mid-cycle IPSPs during a swimming episode can be measured as the percentage of the total number of cycles of the swimming episode on which an IPSP was present. The graph shows that mid-cycle IPSPs occur on all cycles of swimming in motoneurones recorded at positions 0·1–1·7 mm from the otic capsule (segments 2–8). Beyond these positions IPSP reliability declines and IPSPs do not occur at all for activity recorded from motoneurones caudal to the twelfth segment (2·5 mm from the otic capsule).

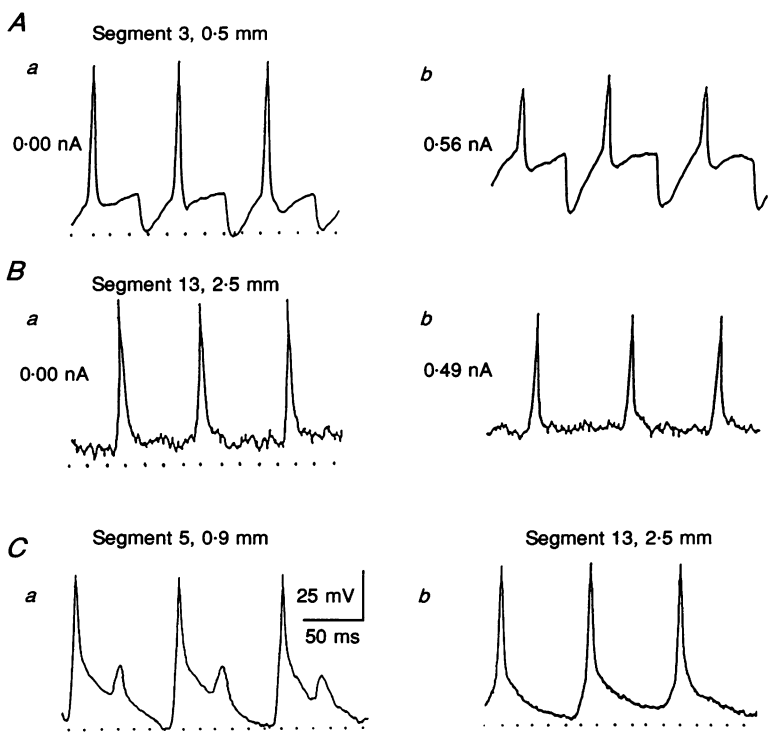

Figure 6. Investigating the presence of mid-cycle IPSPs by the injection of depolarizing current and the use of KCl electrodes
A a, during fictive swimming, prominent IPSPs occurred in a rostral motoneurone recorded at segment 3. *A b*, injection of depolarizing current into this motoneurone resulted in a decrease in the amplitude of the spikes and increased the amplitude of the mid-cycle IPSPs. *Ba*, in a motoneurone recorded at segment 13 IPSPs were absent during fictive swimming. *Bb*, injection of depolarizing current reduced the amplitude of the spikes but failed to reveal the presence of mid-cycle IPSPs. *Ca*, recording from a motoneurone at segment 5 using a KCl-filled electrode. Note that the mid-cycle IPSPs are reversed to become depolarizing. *Cb*, activity recorded from a motoneurone at segment 13 using KCl electrodes fails to reveal the presence of mid-cycle IPSPs. In panels *A–C* the convention for indicating the location from which recordings were made is as described for Fig. 3.

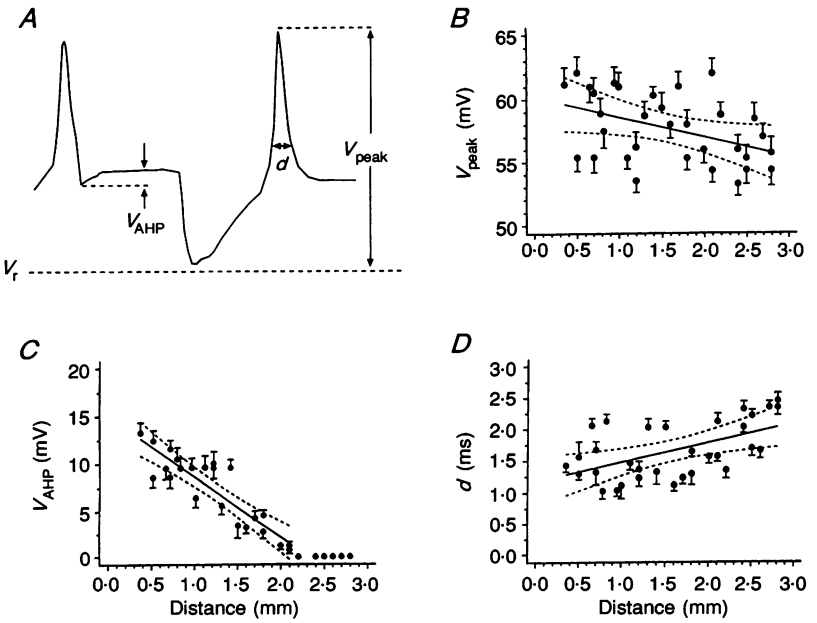

Figure 7. The definition of some features of spikes recorded during fictive swimming and the relationship between these features and spinal position

A, V_{AHP} is the amplitude of the spike after-hyperpolarization and *d* is the spike duration measured at the point of half peak amplitude (V_{peak}). The relationships between spinal position and V_{peak} (*B*), V_{AHP} (*C*) and spike duration (*d*, panel *D*) are all significant ($P < 0.05$). In *B*, *C* and *D* the dashed lines indicate the 95 % confidence limits associated with the line of linear regression. The error bars are the S.D.

current during fictive swimming activity and the second was to record from neurones using KCl-filled electrodes.

Injecting depolarizing current into eight rostral neurones, whose activity showed the presence of IPSPs without current injection, led to an increase in the amplitude of the IPSPs (e.g. Fig. 6*A*). However, injection of current into four neurones located caudal to the twelfth segment failed to reveal the presence of IPSPs (e.g. Fig. 6*B*). Recordings made using KCl electrodes from three neurones located rostral to the twelfth segment revealed reversed IPSPs on cycles of

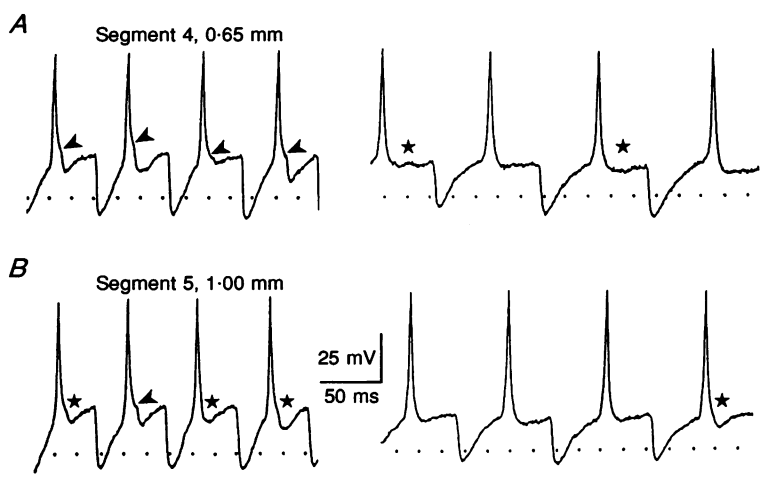

Figure 8. On-cycle inhibition in motoneurones

Recordings from motoneurones at segment 4 (*A*) and segment 5 (*B*). In both cases the beginning and the end of the swimming episode are shown. The arrowheads indicate inflexions in the falling phase of the spike which probably correspond to the turning on of on-cycle IPSPs. The stars indicate cycles where inflexions were not apparent but where the falling phase could be fitted by more than two curves, suggesting that the spike AHP was coincident with an on-cycle IPSP. Note that the incidence of on-cycle IPSPs is higher at the beginning of swimming episodes than at the end.

swimming episodes (e.g. Fig. 6*Ca*), whereas recordings made from two neurones located caudal to the twelfth segment failed to reveal the presence of IPSPs on any cycles (e.g. Fig. 6*Cb*).

Spike properties

Spikes occurring during fictive swimming are non-overshooting, and peak spike amplitudes, measured from the resting potential to the peak of the spike (V_{peak}, Fig. 7*A*), decreased significantly in a rostrocaudal direction ($P < 0{\cdot}05$, Fig. 7*B*). Given that no significant longitudinal trend was found for peak spike amplitudes for current-evoked spikes it is likely that the decline in peak spike amplitudes for spikes occurring during swimming is due to the decline in amplitude of the tonic depolarization.

Of the thirty-two putative motoneurones investigated in this study, in twenty-three, recorded rostral to the tenth post-otic segment, a spike AHP was evident (e.g. Fig. 3*A–C*), whereas in nine motoneurones, recorded caudal to the ninth post-otic segment, no AHP could be detected (e.g. Fig. 3*D*). AHP amplitudes (V_{AHP}, Fig. 7*A*) decreased significantly in a rostrocaudal direction ($P < 0{\cdot}05$, Fig. 7*C*). Spike durations measured at half peak amplitude (*d*, Fig. 7*A*) increased significantly in a rostrocaudal direction ($P < 0{\cdot}05$, Fig. 7*D*). Hence, spikes occurring during fictive swimming in caudal *versus* rostral putative motoneurones have smaller amplitude AHPs, longer durations and smaller peak amplitudes.

On-cycle inhibition

In addition to the prominent phase-locked mid-cycle IPSPs (e.g. filled arrows in Fig. 3), on-cycle IPSPs are also sometimes evident during fictive swimming (Dale, 1985; arrowheads in Fig. 8). These IPSPs occur shortly after a spike at cycle phases less than 0·4, and it has been suggested that they could be mediated by the ipsilateral branches of the commissural (inhibitory) interneurones (Roberts & Clarke, 1982; Dale, 1985). The role of on-cycle IPSPs is uncertain, but it is possible that they could limit multiple firing or contribute to rhythm generation since a single side of the spinal cord, in which the effect of contralateral (mid-cycle) inhibition is absent, can generate rhythm (Kahn & Roberts, 1982; Soffe & Roberts, 1982*b*; Soffe, 1989; Tunstall & Roberts, 1990).

Due to the similarity in the timing of on-cycle IPSPs and spike AHPs, measurement of AHP amplitudes was only performed using cycles where on-cycle inhibition was absent and several criteria were established to distinguish such cycles. Examples of cycles of swimming activity recorded rostral to the eighth post-otic segment where on-cycle IPSPs were absent have been illustrated (e.g. Fig. 3). In many cases on-cycle IPSPs could often be easily distinguished by clear points of inflexion in the voltage–time curve following the spike (e.g. arrowheads in Fig. 8). Another criterion used to select cycles stemmed from the observation, indicated above, that on-cycle IPSPs become less reliable at lower swimming frequencies. This finding is based on the change in the form of the spike falling phase, which is smoother at the end than at the beginning of episodes (e.g. Fig. 8). Since spikes would always be expected to be accompanied by an AHP, such a frequency-related difference in the form of spikes may be due to the failure of on-cycle inhibition at lower swimming frequencies.

An alternative method of distinguishing between cycles with on-cycle IPSPs from those without was to use a quantitative approach based on the number of curves required to fit the spike falling phase. This method depended on the finding that in cases where an on-cycle IPSP was clearly absent (e.g. cycles not indicated by either arrowheads or stars in Fig. 8) the spike falling phase could be fitted by just two exponential curves. However, where an on-cycle IPSP was present (cycles marked by arrowheads in Fig. 8) the falling phase of the spike required up to four curves. This procedure was applied to cycles where it was difficult to determine whether on-cycle IPSPs were present or not (e.g. cycles indicated by stars in Fig. 8).

On-cycle IPSPs were detected on between 20 and 80 % of swimming cycles recorded from putative motoneurones rostral to the eighth post-otic segment. Caudal to the eighth post-otic segment no on-cycle IPSPs could be detected. In cases where they were present the incidence of on-cycle IPSPs decreased as the swimming frequency decreased from the beginning to the end of episodes (e.g. Fig. 8).

DISCUSSION

Intersegmental co-ordination could depend on gradients in neuronal properties or synaptic drive along the spinal cord; the aim of this study has been to determine if such gradients exist. Direct evidence has been presented for longitudinal gradients in neuronal spike duration and AHP properties in putative motoneurones. Perhaps more significantly, we have also shown a longitudinal gradient in excitatory and inhibitory synaptic drive to putative motoneurones during fictive swimming. We have not made any recordings from rhythmically active spinal interneurones, but in other studies made in the rostral spinal cord their pattern of activity during swimming was found to be very similar to motoneurones in the same region (Dale, 1985; Roberts, 1990). If such gradients in synaptic drive were also present in interneurones then they could lead to a longitudinal decline in coupling strength and intrinsic frequency and thereby contribute to the rostrocaudal delay in motor activity observed during fictive swimming (Cohen *et al.* 1982; Kopell, 1988).

As in other vertebrates there is a longitudinal gradient in development in the *Xenopus* embryo. This is clear in the development of gross features of the body such as the muscles or pigmentation (Nieuwkoop & Faber, 1956) and in the differentiation of spinal neurone populations (Dale, Ottersen, Roberts & Storm-Mathisen, 1986; Roberts *et al.* 1988). In such a system we cannot establish whether the gradients that we describe are a functional or developmental feature. This will have to be done by examining adult vertebrates. What seems certain is that the gradients will have significant effects on the longitudinal delays observed during fictive swimming and so presumably also on the properties of the swimming behaviour itself.

Significance of the longitudinal gradients

The way that longitudinal gradients affect the timing of motor discharge will depend on the mechanisms that determine neuronal firing during fictive swimming. At present no direct evidence for endogenous cellular rhythmicity has been obtained in *Xenopus* embryo spinal neurones (N. Dale & S. R. Soffe, personal communication) despite suggestive indirect evidence for its existence (Soffe, 1989). We have therefore concluded that rhythmicity depends importantly on spinal network properties and particularly on rebound from reciprocal inhibition between the two sides of the cord and on recurrent inhibition within each half of the nervous system (Kahn & Roberts, 1982; Soffe, 1989; Roberts & Tunstall, 1990). Such rebound only occurs when neurones are depolarized by excitation and depends on the fact that 80 % of spinal neurones do not fire repetitively when depolarized (Soffe, 1990).

If neurone firing during fictive swimming depends on rebound from inhibition then the interpretation of the longitudinal gradients is complex. In more rostral regions, where excitatory tonic depolarization and mid-cycle IPSPs are large, spikes arise from the falling phase of these IPSPs (see Fig. 3). If mid-cycle IPSPs remained constant, a higher level of excitatory depolarization could bring neurones closer to their firing threshold and may increase the local intrinsic frequency. However, in more rostral regions the IPSPs also become larger and it is not clear whether this will increase or decrease intrinsic frequency. This is because larger IPSPs could increase the effectiveness of post-inhibitory rebound. Mid-cycle IPSPs hyperpolarizing the membrane could have excitatory effects by allowing the deactivation of voltage-gated potassium channels and permitting the reactivation of sodium channels. Both of these processes should lead to an effective increase in intrinsic frequency.

In more caudal regions the situation is more straightforward. The longitudinal decline in the amplitude of both the tonic excitation and the mid-cycle IPSPs could result in a decrease in the efficiency of postinhibitory rebound excitation and consequent fall in intrinsic frequency. IPSPs also have slower rise- and fall-times in caudal neurones and this too may reduce the effectiveness of postinhibitory rebound. However, as IPSPs become smaller caudally it is possible that rebound firing could occur earlier. More caudally still, the mid-cycle IPSPs are absent so rebound can play no part in initiation of firing. This suggests that more caudal neurones (caudal to the twelfth segment 2·4 mm from the midbrain) may be directly driven by excitatory synaptic input from more rostral regions (see below, section on rhythm-generating capacity).

The longitudinal decline in the amplitude of the on-cycle IPSPs may also influence coupling strength and intrinsic frequency since it is a form of recurrent inhibition within each side that could lead to rebound firing in a similar manner to that described for mid-cycle IPSPs. The importance that a gradient in on-cycle IPSPs could have in influencing longitudinal delays would be emphasized in the single-sided preparations, where mid-cycle IPSPs are absent (Kahn & Roberts, 1982; Soffe, 1989).

The rostrocaudal decline in synaptic excitation and inhibition is compatible with anatomical evidence showing that the population density of the excitatory and inhibitory interneurones, that are thought to be active during swimming, declines in a rostrocaudal direction along the spinal cord (excitation: Roberts & Alford, 1986; inhibition: Dale *et al.* 1986; Roberts *et al.* 1988). Since axonal projection distances are usually less than 1 mm for these interneurones, lower neuronal population densities would be expected to lead to fewer synaptic contacts and a consequent reduction in synaptic drive.

For rostrally located neurones both spikes evoked by current and spikes occurring during fictive swimming have shorter durations and larger amplitude AHPs than those in more caudal neurones. One possible explanation for these findings is that K^+ currents decline in a rostrocaudal direction. The rostrocaudal decline in the amplitude of the AHPs could contribute to a general longitudinal decrease in intrinsic frequency by reducing the efficiency of potassium repolarization processes, which would reduce hyperpolarization-dependent sodium channel reactivation. During swimming in neurones caudal to the eighth post-otic segment no AHPs are evident even though they are revealed in the same neurones during current injection. One explanation for this observation is that during swimming there is some kind of synaptically mediated suppression of AHPs in caudal neurones, but further work is needed to ascertain the precise mechanism underlying this finding.

Distribution of rhythm-generating capability

We have shown that the amplitude of the synaptic excitatory and inhibitory drive to neurones during fictive swimming decreases along the spinal circuitry. Earlier studies had shown that progressively more caudal transection of the spinal cord reduces the ability of spinal regions caudal to the transection to sustain fictive swimming, and that transection beyond the fifth post-otic segment eliminates this ability (Kahn & Roberts, 1982; Roberts & Alford, 1986). Related experiments had shown that lower spinal preparations required higher concentrations of bath-applied NMDA to evoke fictive swimming (Soffe & Roberts, 1989). The evidence therefore suggests that both rhythm-generating capability and synaptic drive decline caudally. The spinal cord can be divided into three parts. In the intact animal spinal regions rostral to the fifth post-otic segment appear to possess reliable oscillator capability. Caudal to the fifth post-otic segment the situation is less clear. It seems likely that the region from the fifth to the tenth post-otic segment has sufficient mid-cycle inhibition and receives sufficient excitatory tonic drive from more rostral regions for it to participate actively in rhythm generation. In the absence of external drive these segments cannot generate rhythm.

Regions caudal to the tenth post-otic segment lack mid-cycle inhibition and behave as passive elements which are driven by phasic excitation from more rostral regions. This view suggests that the cord as a whole cannot be regarded as a system of coupled oscillators.

There are, however, some problems with the idea that more caudal spinal regions cannot generate rhythmic oscillations. In a previous paper (Tunstall & Roberts, 1991*b*) we showed that activity recorded from the twelfth post-otic segment could sometimes lead that at the third segment when NMDA was applied caudal to the seventh segment. It is possible that the applied NMDA imparted sufficient additional excitatory drive to the caudal regions to enable them to produce autonomous rhythmic activity. This could have occurred directly, and also indirectly by increasing the drive to regions at segment 7, which in turn led to an increase in the drive to the more caudal regions. In view of the fact that both on-cycle IPSPs and mid-cycle IPSPs are absent during activity recorded from spinal regions caudal to the twelfth segment the nature of rhythm generation in these regions is not clear. However, Soffe (1989) has shown that when one-half of the spinal cord is removed surgically the remaining half spinal cord can generate a few cycles of swimming even in the presence of 10 mM strychnine (i.e. where both mid-cycle and on-cycle inhibition is expected to be blocked) provided Mg^{2+} is present in the saline. This finding raises the possibility that beyond the twelfth segment excitatory drive may enable some rhythm generation to occur in the absence of inhibitory synaptic input.

Relation to other systems

The only other swimming system where a longitudinal gradient has been demonstrated is the leech. Isolation of regions of the nerve cord has shown that there is a caudorostral frequency gradient where frequency increases from the head to the twelfth segment (Pearce & Friesen, 1985*a*). However, caudal to this, isolated regions of nerve cord cannot produce fictive swimming activity, and the reasons for this are not clear (Pearce & Friesen, 1985*a*). In the leech there is no evidence that the frequency gradient is due to a decline in synaptic drive or intersegmental connections (Pearce & Friesen, 1985*a*, *b*). Pearce & Friesen (1988) have concluded that the nature of the intersegmental coupling ensures that a rostrocaudal delay occurs even though there is a caudorostral gradient in intrinsic fictive swimming frequency. The gradients in the leech and *Xenopus* embryos contrast with the findings for the systems controlling crayfish swimmeret beating (Paul & Mulloney, 1986) and lamprey swimming (Cohen, 1987), which showed that ganglia or segments, taken from anywhere along the nervous system, could generate rhythm and furthermore, that there was no systematic longitudinal change in the frequency of this rhythm. However, both these studies are difficult to interpret since rhythm was artificially induced by applied excitants which may activate receptors such as those on sensory pathways that are not activated during normal rhythm generation. Where gradients have been found, in the leech and *Xenopus* preparations, rhythm was evoked by stimulating pathways that normally evoke swimming.

The 'trailing oscillator hypothesis', advanced by Matsushima & Grillner (1990) to explain intersegmental co-ordination in the lamprey suggests that rostrocaudal delays can be obtained by means of a discrete rostral region of high excitability, which then entrains other more caudal regions, all of which possess the same level of excitability. This contrasts with the findings presented in the leech (Pearce & Friesen, 1985*a*, *b*), which showed a continuous decline in oscillator frequency along the nervous system. The data we have presented here suggest that in *Xenopus*, there is also a longitudinal gradient in intrinsic frequency as well as coupling strength. In both the leech and the *Xenopus* embryo the caudal part of the nervous system does not generate rhythm.

Conclusions

The gradients in synaptic excitation and inhibition and in spike and AHP duration and amplitude demonstrated here would be expected to have profound effects on the rostrocaudal delays. We have already shown that changing the gradient artificially changes rostrocaudal delay (Tunstall & Roberts, 1990, 1991). Whether the gradients in synaptic drive provide a sufficient explanation for longitudinal co-ordination is currently being investigated by computer simulations of the spinal networks.

Changes in synaptic drive along the spinal circuitry offer a fast, flexible and reversible means of changing the magnitude and direction of longitudinal delays. Such a mechanism seems in keeping with the fact that survival depends critically on being able to respond quickly and flexibly to sudden and unpredictable stimuli. In the *Xenopus* embryo pinching the head with forceps can lead to a behaviour termed struggling where slower waves of bending pass from the tail to the head (Soffe, 1991). Fictive struggling is characterized by bursts of ventral root activity which occur with caudorostral delay (Soffe, 1991). The reversal in the direction of co-ordination that occurs during struggling may be explained by an increase in the excitatory drive in more caudal regions leading to an increase in intrinsic frequency and coupling strength and thereby permitting caudal neurones to fire before their rostral neighbours.

REFERENCES

BUCHANAN, J. T. (1992). Neural network simulations of coupled locomotor oscillators in the lamprey spinal cord. *Biological Cybernetics* **66**, 367–374.

BUCHANAN, J. T., GRILLNER, S., CULLHEIM, S. & RISLING, M. (1989). Identification of excitatory interneurons contributing to generation of locomotion in lamprey, structure, pharmacology, and function. *Journal of Neurophysiology* **62**, 59–69.

COHEN, A. H. (1987). Effects of oscillator frequency on phase-locking in the lamprey central pattern generator. *Journal of Neuroscience Methods* **21**, 113–125.

COHEN, A. H., HOLMES, P. J. & RAND, R. H. (1982). The nature of the coupling between segmental oscillators of the lamprey spinal generator for locomotion: a mathematical model. *Journal of Mathematical Biology* **13**, 345–369.

COHEN, A. H. & WALLEN, P. (1980). The neuronal correlate of locomotion in fish: "Fictive swimming" induced in an *in vitro* preparation of the lamprey spinal cord. *Experimental Brain Research* **41**, 11–18.

DALE, N. (1985). Reciprocal inhibitory interneurones in the *Xenopus* embryo spinal cord. *Journal of Physiology* **363**, 61–70.

DALE, N., OTTERSEN, O. P., ROBERTS, A. & STORM-MATHISEN, J. (1986). Inhibitory neurones of a motor pattern generator in *Xenopus* revealed by antibodies to glycine. *Nature* **324**, 255–257.

DALE, N. & ROBERTS, A. (1984). Excitatory amino acid receptors in *Xenopus* embryo spinal cord and their role in the activation of swimming. *Journal of Physiology* **348**, 527–543.

DALE, N. & ROBERTS, A. (1985). Dual-component amino acid-mediated synaptic potentials, excitatory drive for swimming in *Xenopus* embryos. *Journal of Physiology* **363**, 35–59.

FRIESEN, W. O. (1989). Neuronal control of leech swimming movements. In *Neuronal and Cellular Oscillators*, ed. JACKLET, J. W., pp. 269–315. Marcel Dekker, New York and Basel.

GRILLNER, S. (1974). On the generation of swimming in the spinal dogfish. *Experimental Brain Research* **20**, 459–470.

GRILLNER, S., BUCHANAN, J. T., WALLEN, P. & BRODIN, L. (1988). Neural control of locomotion in vertebrates. In *Neural Control of Rhythmic Movements in Vertebrates*, ed. COHEN, A. H., ROSSIGNOL, S. & GRILLNER, S., pp. 1–40. Wiley, New York.

GRILLNER, S., PERRET, C. & ZANGGER, P. (1976). Central generation of locomotion in the spinal dogfish. *Brain Research* **109**, 255–269.

IKEDA, K. & WIERSMA, C. A. G. (1964). Autogenic rhythmicity in the abdominal ganglia of the crayfish: the control of swimmeret movements. *Comparative Biochemistry and Physiology* **12**, 107–115.

KAHN, J. A. & ROBERTS, A. (1982). Experiments on the central pattern generator for swimming in amphibian embryos. *Philosophical Transactions of the Royal Society* B **296**, 229–243.

KOPELL, N. (1988). Towards a theory of modelling central pattern generators. In *Neural Control of Rhythmic Movements in Vertebrates*, ed. COHEN, A. H., ROSSIGNOL, S. & GRILLNER, S., pp. 369–413. Wiley, New York.

MATSUSHIMA, T. & GRILLNER, S. (1990). Intersegmental co-ordination of undulatory movements – a "trailing oscillator" hypothesis. *NeuroReport* **1**, 97–100.

MATSUSHIMA, T. & GRILLNER, S. (1992). Neural mechanisms of intersegmental coordination in the lamprey: local excitability changes modify phase coupling along the spinal cord. *Journal of Neurophysiology* **67**, 373–388.

NIEUWKOOP, P. D. & FABER, J. (1956). *Normal Tables of Xenopus laevis (Daudin)*. Elsevier, North-Holland, Amsterdam.

PAUL, D. H. & MULLONEY, B. (1986). Intersegmental coordination of swimmeret rhythms in isolated nerve cords of crayfish. *Journal of Comparative Physiology* A **158**, 215–224.

PAVLIDIS, T. (1973). *Biological Oscillators, Their Mathematical Analysis*. Academic Press, New York, .

PEARCE, R. A. & FRIESEN, W. O. (1984). Intersegmental coordination of leech swimming: comparison of in situ and isolated nerve cord activity with body wall movement. *Brain Research* **299**, 363–366.

PEARCE, R. A. & FRIESEN, W. O. (1985*a*). Intersegmental coordination of the leech swimming rhythm. I. Roles of period gradient and coupling strength. *Journal of Neurophysiology* **58**, 1444–1459.

PEARCE, R. A. & FRIESEN, W. O. (1985*b*). Intersegmental coordination of the leech swimming rhythm. II. Comparison of long and short chains of ganglia. *Journal of Neurophysiology* **58**, 1460–1472.

PEARCE, R. A. & FRIESEN, W. O. (1988). A model for intersegmental coordination in the leech nerve cord. *Biological Cybernetics* **58**, 301–311.

ROBERTS, A. (1990). How does a nervous system produce behaviour? A case study in neurobiology. *Science Progress* **74**, 31–51.

ROBERTS, A. & ALFORD, S. T. (1986). Descending projections and excitation during fictive swimming in *Xenopus* embryos: neuroanatomy and lesion experiments. *Journal of Comparative Neurology* **250**, 253–261.

ROBERTS, A. & CLARKE, J. D. W. (1982). The neuroanatomy of an amphibian embryo spinal cord. *Philosophical Transactions of the Royal Society* B **296**, 195–212.

ROBERTS, A., DALE, N., OTTERSEN, O. P. & STORM-MATHISEN, J. (1988). Development and characterization of commissural interneurones in the spinal cord of *Xenopus laevis* embryos revealed by antibodies to glycine. *Development* **103**, 447–461.

ROBERTS, A. & KAHN, J. A. (1982). Intracellular recordings from spinal neurones during "swimming" in paralysed amphibian embryos. *Philosophical Transactions of the Royal Society* B **296**, 213–228.

ROBERTS, A. & TUNSTALL, M. J. (1990). Mutual re-excitation with post-inhibitory rebound, a simulation study on the mechanisms for locomotor rhythm generation in the spinal cord of *Xenopus* embryos. *European Journal of Neuroscience* **2**, 11–23.

ROVAINEN, C. M. (1986). The contributions of multisegmental interneurons to the longitudinal coordination of fictive swimming in the lamprey. In *Neurobiology of Vertebrate Locomotion*, ed. GRILLNER, S., STEIN, P. S. G., STUART, D. G., FORSSBERG, H. & HERMAN, R. M., pp. 321–334. Macmillan, London.

SILLAR, K. T. & ROBERTS, A. M. (1988). Unmyelinated cutaneous afferent neurons activate two types of excitatory amino-acid receptor in the spinal cord of *Xenopus laevis* embryos. *Journal of Neuroscience* **8**, 1350–1360.

SOFFE, S. R. (1987). Ionic and pharmacological properties of reciprocal inhibition in *Xenopus* embryo motoneurones. *Journal of Physiology* **382**, 463–473.

SOFFE, S. R. (1989). Roles of glycinergic inhibition and *N*-methyl-D-aspartate receptor mediated excitation in the locomotor rhythmicity of one half of the *Xenopus* embryo central nervous system. *European Journal of Neuroscience* **1**, 561–571.

SOFFE, S. R. (1990). Active and passive membrane properties of spinal cord neurones which are rhythmically active during swimming in *Xenopus* embryos. *European Journal of Neuroscience* **2**, 1–10.

SOFFE, S. R. (1991). Triggering and gating of motor responses by sensory stimulation, behavioural selection in *Xenopus* embryos. *Proceedings of the Royal Society* B **246**, 197–203.

SOFFE, S. R., CLARKE, J. D. W. & ROBERTS, A. (1984). Activity of commissural interneurons in spinal cord of *Xenopus* embryos. *Journal of Neurophysiology* **51**, 1257–1267.

SOFFE, S. R. & ROBERTS, A. (1982*a*). Activity of myotomal motoneurons during fictive swimming in frog embryos. *Journal of Neurophysiology* **48**, 1274–1278.

SOFFE, S. R. & ROBERTS, A. (1982*b*). Tonic and phasic synaptic input to spinal cord motoneurones during fictive swimming in frog embryos. *Journal of Neurophysiology* **48**, 1279–1288.

SOFFE, S. R. & ROBERTS, A. (1989). The influence of magnesium ions on the NMDA mediated responses of ventral rhythmic neurones in the spinal cord of *Xenopus* embryos. *European Journal of Neuroscience* **1**, 507–515.

STEIN, P. S. G. (1976). Mechanisms of interlimb phase control. In *Neural Control of Locomotion*, ed. HERMAN, R. M., GRILLNER, S., STEIN, P. S. G. & STUART, D. G., pp. 465–487. Plenum Press, New York.

TUNSTALL, M. J. & ROBERTS, A. (1990). NMDA applied to the spinal cord of *Xenopus* embryos reduces rostral-caudal delay during fictive swimming. *Journal of Physiology* **425**, 92*P*.

TUNSTALL, M. J. & ROBERTS, A. (1991*a*). Experiments on the neural basis of the rostro-caudal delay during swimming in *Xenopus* embryos. *Journal of the Marine Biological Association* **71**, 3.

TUNSTALL, M. J. & ROBERTS, A. (1991*b*). Longitudinal co-ordination of motor output during swimming in *Xenopus* embryos. *Proceedings of the Royal Society* B **244**, 27–32.

WALLEN, P. & WILLIAMS, T. L. (1982). Intersegmental coordination in the isolated spinal cord of the lamprey during 'fictive locomotion' as compared with swimming in the intact and spinal lamprey. *Journal of Physiology* **325**, 30–31*P*.

WILLIAMS, T. L. (1992). Phase coupling in simulated chains of coupled oscillators representing the lamprey spinal cord. *Neural Computation* **4**, 546–558.

WILLIAMS, T. L., SIGVARDT, K., KOPELL, N., ERMENTROUT, G. B. & REMLER, M. P. (1990). Forcing of coupled non-linear oscillators. Studies of intersegmental coordination in the lamprey locomotor central pattern generator. *Journal of Neurophysiology* **64**, 862–871.

Acknowledgements

This work was supported by the Science and Engineering Research Council. We would like to thank Drs N. Dale, W. J. Heitler, R. W. Meech, S. R. Soffe and T. L. Williams for critical comments on the manuscript and M. R. Gamble for technical assistance.

Author's present address

M. J. Tunstall: Neuroscience Centre, University of Otago, Dunedin, New Zealand.

Received 17 November 1992; accepted 15 July 1993.